

Nonlinear photonic lattices in anisotropic nonlocal self-focusing media

Anton S. Desyatnikov, Dragomir N. Neshev, and Yuri S. Kivshar

Nonlinear Physics Centre and Centre for Ultra-High bandwidth Devices for Optical Systems (CUDOS),
Research School of Physical Sciences and Engineering, Australian National University,
Canberra, ACT 0200, Australia

Nina Sagemerten, Denis Träger, Johannes Jägers, and Cornelia Denz

Institute of Applied Physics, Westfälische Wilhelms-Universität Münster, D-48149 Münster, Germany

Yaroslav V. Kartashov

ICFO—Institut de Ciències Fotòniques and Department of Signal Theory and Communications,
Universitat Politècnica de Catalunya, 08034 Barcelona, Spain

Received October 19, 2004

We analyze theoretically and generate experimentally two-dimensional nonlinear lattices with periodic phase modulation in a photorefractive medium. The light-induced periodically modulated nonlinear refractive index is highly anisotropic and nonlocal, and it depends on the lattice orientation relative to the crystal axis. We discuss the stability of such induced photonic structures and their guiding properties. © 2005 Optical Society of America

OCIS codes: 190.4420, 190.5530.

The study of nonlinear effects in periodic photonic structures recently attracted strong interest because of the many novel possibilities for controlling light propagation, steering, and trapping. Periodic modulation of the refractive index modifies the linear spectrum and wave diffraction and consequently strongly affects the nonlinear propagation and localization of light.¹

Photonic lattices can be optically induced by linear diffraction-free light patterns created by the interference of several plane waves.² However, the induced change in the refractive index depends on the light intensity, and in the nonlinear regime it is accompanied by the self-action effect.³ The nonlinear diffraction-free light patterns in the form of stable self-trapped periodic waves can propagate without change in their profile, becoming the eigenmodes of the self-induced periodic potentials. This behavior is generic since nonlinear periodic waves can exist in many types of of nonlinear system, and they provide a simple realization of nonlinear photonic crystals. Such structures are flexible because the lattice is modified and shaped by the nonlinear medium; these flexible lattices extend the concept of optically induced gratings beyond the limits of weak material nonlinearity. Moreover, nonlinear lattices offer many novel possibilities for the study of nonlinear effects in periodic systems because they can interact with localized signal beams through cross-phase modulation and form composite bound states.^{4,5}

Nonlinear photonic lattices created by two-dimensional arrays of pixel-like solitons were recently demonstrated experimentally in parametric processes⁶ and in photorefractive crystals with both coherent⁷ and partially incoherent^{3,5,8} light. For the case of two-dimensional arrays of in-phase solitons created by amplitude modulation, every pixel of the

lattice induces a waveguide that can be manipulated by an external steering beam.^{7–9} However, the spatial periodicity of these lattices is limited by the attractive soliton interaction that may lead to their strong instability. In contrast, the recently suggested two-dimensional lattices of out-of-phase solitons are known to be robust in an isotropic saturable model.¹⁰ The phase profile of such self-trapped waves resembles a chessboard with the lines of π -phase jumps between neighboring white and black sites.

In this Letter we study two-dimensional nonlinear lattices with a chessboard phase structure in anisotropic nonlocal self-focusing media and generate such lattices experimentally in a photorefractive crystal. We demonstrate that the light-induced periodically modulated nonlinear refractive index is highly anisotropic and nonlocal, and it depends on the lattice orientation relative to the crystal axis. We discuss the stability of such induced photonic structures and their guiding properties. An advantage of using this novel type of nonlinear periodic lattice when compared with in-phase lattices or incoherent soliton arrays^{3,7} is that such lattices can be made robust even with smaller lattice spacing.

Spatially periodic nonlinear modes appear naturally because of the self-focusing effect and modulational instability.¹ When self-focusing compensates for the diffraction of optical beams, it may support both isolated spatial solitons and periodic soliton trains or stationary periodic nonlinear waves. The latter include the well-studied cnoidal waves, solutions to the nonlinear Schrödinger equation,

$$i\partial_z E + \nabla_{\perp}^2 E + n(I)E = 0, \quad (1)$$

where $I \equiv |E|^2$ and $\nabla_{\perp}^2 = \partial_x^2 + \partial_y^2$. Similar stable periodic waves exist in different nonlinear models, including quadratic and Kerr-type saturable nonlinearities.

The family of two-dimensional nonlinear periodic waves¹⁰ can also be extended to the case of rectangular geometry with two different transverse periods because such anisotropic deformations of the square lattice do not enhance its modulational instability. Stabilization of phase-engineered soliton arrays was reported recently for an anisotropic model.⁹

In this Letter we consider photorefractive crystal as an example of an anisotropic and nonlocal nonlinear medium. In this case the nonlinear contribution to the refractive index in Eq. (1) is given by¹¹

$$n(I) = \Gamma \partial_x \varphi, \quad (2)$$

where electrostatic potential φ of the optically induced space-charge field satisfies a separate equation:

$$\nabla_{\perp}^2 \varphi + \nabla_{\perp} \varphi \nabla_{\perp} \ln(1+I) = \partial_x \ln(1+I). \quad (3)$$

Here intensity I is measured in units of the background illumination (dark) intensity necessary for the formation of spatial solitons in such a medium. Physical variables \tilde{x} , \tilde{y} , and \tilde{z} correspond to their dimensionless counterparts as $(\tilde{x}, \tilde{y}) = x_0(x, y)$ and $\tilde{z} = 2\kappa x_0^2 z$, where x_0 is the transverse scale factor and $\kappa = 2\pi n_0/\lambda$ is the carrier wave vector with linear refractive index n_0 . Parameter $\Gamma = x_0^2 \kappa^2 n_0^2 r_{\text{eff}} \mathcal{E}$ is defined through effective electro-optic coefficient r_{eff} and externally applied bias electrostatic field \mathcal{E} .

Stationary solutions to the system of Eqs. (1)–(3) are sought in the standard form $E(x, y, z) = U(x, y) \exp(ikz)$, where real envelope U satisfies the equation

$$-kU + \nabla_{\perp}^2 U + \Gamma \partial_x \varphi U = 0. \quad (4)$$

We look for periodic solutions, $U(X, Y) = U(X + 2\pi, Y + 2\pi)$, and solve Eqs. (3) and (4) using the relaxation technique¹¹ with the initial ansatz in the form of a linear periodic mode, $U_{\text{lin}}(X, Y) = A \sin X \sin Y$. We find that at least two distinct families bifurcate from linear wave U_{lin} , depending on its orientation: a square pattern parallel to the c axis with $(X, Y) = (x, y)$ and a diamond pattern oriented diagonally with $(X, Y) = (x \pm y)/\sqrt{2}$. Figures 1(a) and 1(b) show the field and refractive-index distributions in the low ($k = -1.9$, $A \approx 0.9$) and relatively high ($k = -1.5$, $A \approx 3.6$) saturation regimes for both families. In the general case of $\Gamma \neq 1$, these two families occupy a band $k \in [-2, \Gamma - 2]$ with amplitudes $A(k)$ and power densities $P(k)$ vanishing in the linear limit $k \rightarrow -2$ [see Fig. 1(c)]. Here the power density is defined as the power of a unit cell, $P = 4 \iint_0^{\pi} U^2 dX dY$. The main difference between the two solutions, clearly seen in Figs. 1(a) and 1(b), comes from the refractive index: The regions with the effective focusing lenses are well separated for the diamonds and fuse to the effectively one-dimensional stripes for the square pattern in the limit of strong saturation. In Fig. 1(c) we plot maximal and minimal values (extrema) of the refractive index, $\text{Ext}(\partial_x \varphi)$.

In Fig. 1(d) we show the FWHM of a single intensity spot in two orthogonal directions $d_{x,y}$ characterizing the degree of spatial localization of a cnoidal wave.¹⁰ The ellipticity of every lattice site, $\epsilon = d_y/d_x \geq 1$, depends on propagation constant k , similar to the ellipticity of a single photorefractive soliton¹¹ [see Fig. 1(d)].

To test the lattice stability, we propagate numerically two types of initially perturbed periodic solution and observe robust propagation for the distances exceeding the experimental crystal length. Figure 2 demonstrates an example of stable propagation for the parameters close to our experimental situation.

To demonstrate experimentally both the existence and the stability of these nonlinear periodic lattices in anisotropic and nonlocal media, we use a setup similar to that employed in Ref. 5. A linearly polarized beam from a frequency-doubled Nd:YAG laser at 532 nm is sent to a liquid-crystal programmable spatial light modulator to create a periodic light pattern with a variable period and orientation. The output of the modulator is then imaged by a high-numerical-aperture telescope (demagnification of ~ 10) on the front face of a 2.3-cm-long photorefractive SBN:60 crystal. The incident light is linearly polarized parallel to the c axis, thus experiencing strong photorefractive nonlinearity. The imposed pure phase modulation transforms into an amplitude modulation of the beam at the front face of the crystal, where noise is reduced by proper spatial filtering. The crystal is externally biased and uniformly illuminated with a white light to control the dark irradiance. The gener-

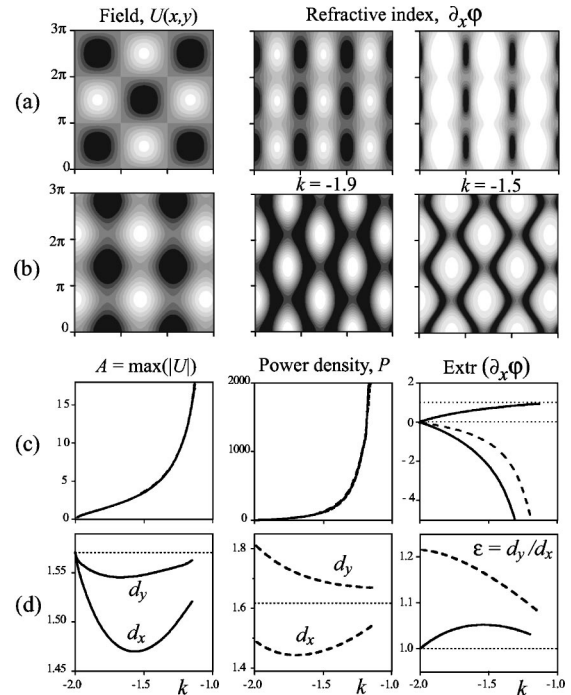


Fig. 1. (a) Square and (b) diamond self-trapped stationary periodic patterns in the model in Eqs. (1)–(3) at $\Gamma = 1$. Families of nonlinear waves are summarized in (c) and (d); solid (dashed) curves correspond to the square (diamond) patterns. Both lines for A , P , and $\text{max}(\partial_x \varphi)$ coincide in (c). Horizontal dotted lines in (d) correspond to the linear limit $\Gamma \rightarrow 0$.

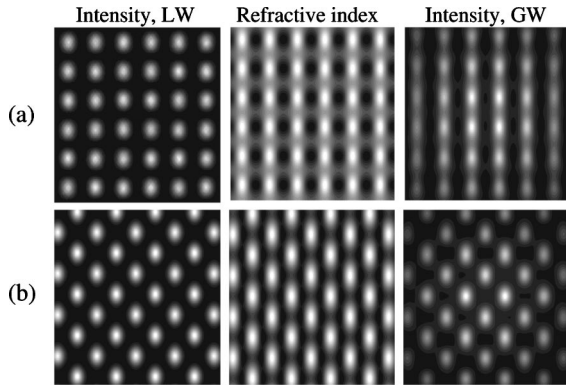


Fig. 2. Numerical results for the propagation of (a) square and (b) diamond self-trapped patterns for $\Gamma=11.8$ in the low-saturation regime with $A \approx 1$ and $k=-0.5$. Intensities of the lattice wave (LW) and the probe wave it guides (GW) are shown after propagation of $\tilde{z} \approx 23$ mm. On the input the lattice is perturbed by 20% of the random noise, and the probe is a broad Gaussian beam.

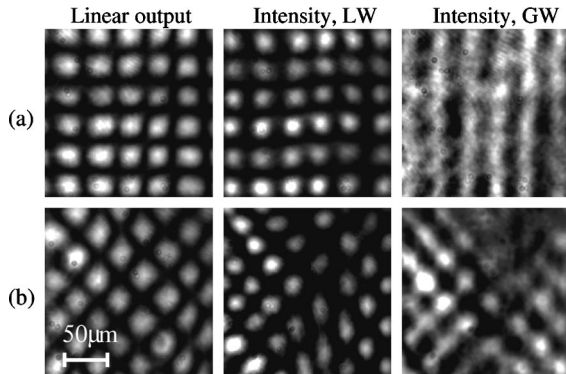


Fig. 3. Experimental results for the (a) square and (b) diamond lattices. Left to right, output intensities of the lattice after linear and nonlinear propagation and output of a guided plane wave.

ated periodic pattern represents a nondiffracting beam and experiences robust linear propagation in the crystal (at zero bias) with a negligible change in the periodicity. The input of the generated periodic wave is therefore identical to the linear output. A typical example of the intensity pattern with a periodicity of $31 \mu\text{m}$ at the back face of the crystal is shown in Fig. 3 (left column) for two different orientations with respect to the crystal axis.

Applying an external dc electric field ($\mathcal{E}=1000 \text{ V/cm}$) across the crystal provides appropriate conditions for the formation of a single spatial soliton of $\sim 15\text{-}\mu\text{m}$ size. Such a high voltage (nonlinearity) influences the propagation of the periodic waves; however, the output of the lattice does not change qualitatively [Fig. 3 (middle column)]. Therefore the only way to test whether the lattice propagates truly nonlinearly is to probe whether it induces changes in the crystal refractive index. To test this, we send a broad plane wave through the crystal and observe its modulation at the output. In practice, this is realized by switching off the voltage on the modulator, thus removing the modulation imposed on the light pattern and generating a broad plane wave at the input

of the crystal. This approach ensures that the plane wave is propagating exactly along the induced waveguides. Because of the slow response of the photorefractive crystal, we can quickly monitor the output of the plane wave without modifying the induced refractive-index change. Output intensity distributions for two orientations of the lattice pattern are shown in Fig. 3 (right column). The plane wave is indeed modulated by the induced periodic potential, and we observe guiding of the probe beam at the maxima of the refractive index. Besides inhomogeneities in the periodic pattern, the experimental pictures shown in Fig. 3 are in a good agreement with the corresponding numerical simulations presented in Fig. 2 and demonstrate a qualitative difference in the guided patterns for two different orientations of the lattice. Closely related anisotropic enhancement of discrete diffraction was demonstrated recently by Chen *et al.*¹²

In conclusion, we have studied theoretically and generated experimentally two-dimensional nonlinear photonic lattices in an anisotropic photorefractive medium. We have found two distinct classes of self-trapped robust spatially periodic waves with out-of-phase neighboring sites, the square pattern oriented parallel to the crystal axes, and the diamond pattern oriented diagonally in the transverse plane. We have demonstrated that the highly anisotropic refractive-index distribution induced by the lattice differs significantly from its isotropic counterpart and depends strongly on the lattice orientation.

The authors acknowledge fruitful discussions with Z. Chen and W. Krolkowski. This work was supported by the Australian Research Council, the Alexander von Humboldt Foundation, and the Deutsche Forschungsgemeinschaft in the frame of the graduate school “Nonlinear Continuous Systems”.

References

1. Yu. S. Kivshar and G. P. Agrawal, *Optical Solitons: from Fibers to Photonic Crystals* (Academic, San Diego, Calif., 2003).
2. J. W. Fleischer, M. Segev, N. K. Efremidis, and D. N. Christodoulides, *Nature* **422**, 147 (2003).
3. Z. Chen and K. McCarthy, *Opt. Lett.* **27**, 2019 (2002).
4. A. S. Desyatnikov, E. A. Ostrovskaya, Yu. S. Kivshar, and C. Denz, *Phys. Rev. Lett.* **91**, 153902 (2003).
5. D. Neshev, Yu. S. Kivshar, H. Martin, and Z. G. Chen, *Opt. Lett.* **29**, 486 (2004).
6. S. Minardi, S. Sapone, W. Chinaglia, P. Di Trapani, and A. Berzanskis, *Opt. Lett.* **25**, 326 (2000).
7. J. Petter, J. Schröder, D. Träger, and C. Denz, *Opt. Lett.* **28**, 438 (2003).
8. H. Martin, E. D. Eugenieva, Z. Chen, and D. N. Christodoulides, *Phys. Rev. Lett.* **92**, 123902 (2004).
9. M. Petrović, D. Träger, A. Strinić, M. Belić, J. Schröder, and C. Denz, *Phys. Rev. E* **68**, 055601R (2003).
10. Y. V. Kartashov, V. A. Visloukh, and L. Torner, *Phys. Rev. E* **68**, 015603 (2003).
11. A. A. Zozulya, D. Z. Anderson, A. V. Mamaev, and M. Saffman, *Phys. Rev. A* **57**, 522 (1997).
12. Z. Chen, H. Martin, E. D. Eugenieva, J. Xu, and A. Bezryadina, *Phys. Rev. Lett.* **92**, 143902 (2004).